analytical chemistry

pubs.acs.org/ac Article

Online Coupling of Liquid Chromatography with Fourier Transform Ion Cyclotron Resonance Mass Spectrometry at 21 T Provides Fast and Unique Insight into Crude Oil Composition

Steven M. Rowland,[‖] Donald F. Smith,[‖] Gregory T. Blakney, Yuri E. Corilo, Christopher L. Hendrickson, and Ryan P. Rodgers*

Cite This: *Anal. Chem.* 2021, 93, 13749−13754 Read Online

ACCESS | Metrics & More | Article Recommendations | Supporting Information

ABSTRACT: High magnetic field Fourier transform ion cyclotron resonance (FT-ICR) mass spectrometry provides the highest mass resolving power and mass measurement accuracy for detailed characterization of complex chemical mixtures. Here, we report the coupling of online liquid chromatography of complex mixtures with a 21 tesla FT-ICR mass spectrometer. The high magnetic field enables large ion populations to be analyzed for each spectrum for a high dynamic range, with 3.2 million mass resolving power at m/z 400 (6.2 s transient duration) or 1.6 million (3.1 s transient duration) while maintaining high mass accuracy for molecular formula assignment (root-mean-square assignment error < 0.150 ppm). Thousands of unique elemental compositions are assigned *per mass spectrum*, which can be grouped by the heteroatom class, double bond equivalents (the number of rings and double bonds to carbon), and carbon number. Figures of merit are discussed, as well as characterization of an Arabian heavy vacuum gas oil in terms of the ring number, compound class, double bond equivalents, and ion type. Consideration of elemental composition and retention order provides additional structural information.

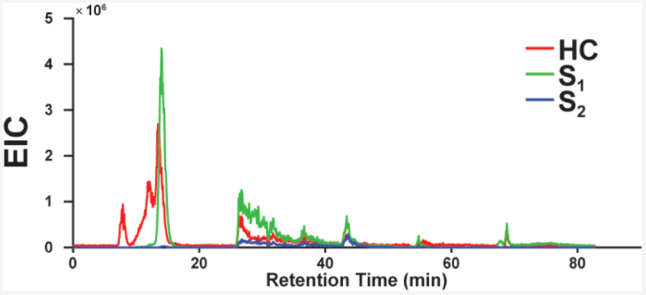

INTRODUCTION

High-field Fourier transform ion cyclotron resonance mass spectrometry (FT-ICR MS) enables detailed chemical characterization of crude oil and petroleum-derived samples. Samples are typically examined by direct infusion, which enables chemical compositional assignment of tens of thousands of ions from these complex samples. Further, methods to increase the compositional coverage over traditional direct infusion have been developed. Off-line fractionation has also been employed along with FT-ICR mass spectrometry to understand the composition of petroleum samples, especially with regard to less volatile components such as heavy distillates and polar compounds. Acidic compounds are easily extracted by ion-exchange resins or amine-based stationary phases, and extractions may even be modified to separate acids by molecular weight.[1−3] Other compound classes, including basic nitrogen, sulfides, and petroporphyrins, have also been isolated and identified by the combination of off-line chromatography with high-resolution mass spectrometry.[4−10] More recently, an exhaustive technique to detect multiple petroleum families was described and utilized off-line fractionation with high-resolution mass spectrometry.[11]

Over the past decade, advances in both ionization techniques and high-resolution mass spectrometers have led to the coupling of chromatography and high-resolution mass spectrometry for the analysis of ultracomplex samples. Schrader et al. have published a series of works that utilize online liquid chromatography−mass spectrometry (LC-MS) to study both crude oils and asphaltenes.[12−15] Robson and co-workers showed good separation of nitrogen compounds after off-line fractionation, thereby showing the need for the combined resolution of online LC-MS for a complex mixture analysis.[11] More recently, Gavard *et al.* reported a software suite, Kairos MS, for processing of hyphenated ultra-high-resolution mass spectrometry data. Trends for oxygen-containing compounds for gas chromatography−atmospheric pressure chemical ionization (GC-APCI) FT-ICR of oil sand processing water and two groundwater samples were shown, as well as liquid chromatography−electrospray ionization (LC-ESI) Orbitrap of two dissolved organic matter samples.[16] Despite the recent success, the complexity of heavy oil samples, combined with the generation of more than one ion type by

Received: March 17, 2021
Accepted: September 22, 2021
Published: October 8, 2021

https://doi.org/10.1021/acs.analchem.1c01169
Anal. Chem. 2021, 93, 13749−13754

APPI, demands ultrahigh resolving power and mass accuracy for proper characterization of these complex organic mixtures.

Mass resolving power improves linearly, and mass accuracy, dynamic range, and charge capacity (before peak coalescence) improve quadratically with magnetic field strength for FT-ICR MS. Thus, high magnetic field FT-ICR MS alleviates limitations that hamper the online LC-MS analysis of complex mixtures. A recent work by Smith and co-workers shows a better than 2-fold improvement in root-mean-square (RMS) assignment error at 21 T when compared to FT-ICR MS at 9.4 T for direct infusion experiments.[17] Similarly, the 21 T mass spectrometer consistently revealed greater numbers of molecular formula assignments across a wide range of samples and ionization modes. Mass resolving power ($m/\Delta m_{50\%}$) > 2 700 000 at m/z 400 was demonstrated, which enabled the resolution of mass differences as low as 0.53 mDa at m/z 677.

Here, we present a chromatographic separation based on the aromatic ring class,[18] in combination with the ultrahigh mass resolving power of FT-ICR MS at 21 T. The high magnetic field provides the necessary dynamic range, mass resolving power, and mass accuracy for high-level analysis of each chromatographic scan and enables data collection at chromatographic time scales. A transient duration of 3.1 s yields absorption mode mass spectra with $m/\Delta m_{50\%}$ = 1 600 000, which is sufficient to mass resolve the common 1.1 mDa mass difference ($S_1H_3{}^{13}C_1$ versus C_4) observed by atmospheric pressure photoionization (APPI) up to ~m/z 700. We describe the figures of merit for this type of analysis and show insights into a chemical structure that is only possible through online LC-MS analysis.

EXPERIMENTAL SECTION

Reagents and Samples. Solvents used (*n*-heptane, dichloromethane, isopropyl alcohol, acetonitrile, and toluene) were of high-performance liquid chromatography (HPLC) grade and used as received (J.T. Baker Chemicals, Swedesboro, NJ). Two samples were analyzed: Arabian heavy gas oil distillate (371−510 °C) and Mackay Canadian bitumen distillate (550−600 °C).

Fourier Transform Ion Cyclotron Resonance Mass Spectrometry at 21 T. Mass spectral analysis was performed with a custom-designed 21 T FT-ICR MS.[17,19] Large ion populations (1−3 × 10^6 charges) were accumulated in a Velos Pro linear ion trap (Thermo Scientific, San Jose, CA), transferred to an external linear quadrupole ion trap, followed by auxiliary RF ejection[20] to a dynamically harmonized ICR cell[21] operated at 6 volts trapping potential. A Predator data station was used for ion excitation and detection, with 3.1 or 6.2 s transient duration for the LC analysis.[22] For direct infusion, fractions were diluted in toluene to 50 μg/mL and 100 scans were signal averaged using a 3.1 s transient duration with AGC targets of 0.4−1.0 × 10^6. The instrument was operated in positive-ion mode with atmospheric pressure photoionization (APPI) and a scan range of 150−2000 Th for all experiments.

Liquid Chromatography. The chromatographic separation utilizes a previously reported dual-column separation based on the aromatic ring class.[18] Liquid chromatography was performed with a Waters Alliance e2695 (Waters, Milford, MA). The first column was a 4.6 × 250 mm^2 Chromegabond 2,4-dinitroanilinopropyl silica (DNAP) analytical column with 5 μm particle size (ES Industries, West Berlin, NJ) and was utilized to separate 1−5-ring hydrocarbons and polar compounds. The second column was a 4.6 × 250 mm^2 Spherisorb strong cation exchange (SCX) column with a 5 μm particle size (Waters, Milford, MA). The SCX column was converted into a silver-impregnated cation exchange column prior to use by flushing with a 30 mg/mL solution of silver nitrate in acetonitrile, followed by pure acetonitrile, dichloromethane, and hexane. This separation utilized a complex four-solvent system with switching valves to control the mobile phase composition through each column. This method was used exactly as previously reported, and the solvent composition (at pump) and column timing are shown in Supporting Information (SI) Table S1. A fraction collector was used to collect samples for the direct infusion analysis. For online analysis, approximately 125 μg of petroleum was loaded on the column, and a 10:1 split postcolumn (toluene) resulted in ~11 μg of total sample injected into the mass spectrometer.

Data Analysis and Visualization. All spectra were phase-corrected[23] and internally calibrated with respect to a homologous series with high relative abundance. For LC-MS, a master peak list was assembled and elemental compositions were assigned with PetroOrg.[24] The in-house developed MATLAB scripts (R2018 v9.4.0.813654; Mathworks, Natick, MA) were used to match elemental compositions with the observed m/z values using a tolerance of ±0.5 ppm and to create extracted ion chromatograms (EICs) for class and double bond equivalents (DBEs; the number of rings plus double bonds to carbon). Signal magnitude was normalized with respect to the inject time (IT) using eq 1.

$$\text{signal magnitude}_{\text{normalized}} = \frac{\text{signal magnitude}_{\text{measured}}}{\text{IT}} \times 1000 \quad (1)$$

RESULTS AND DISCUSSION

Figures of Merit. Analysis of crude oil and petroleum distillates by LC-FT-ICR MS provides a wealth of information with regard to the chemical composition of a sample in a relatively short analysis time compared to other methods, such as off-line fractionation prior to the high-resolution MS analysis. The work presented here demonstrates the power of LC-MS with ultra-high-resolution mass spectrometry to provide chemical and structural information for petroleum samples. This work also aims to demonstrate the figures of merit associated with online LC-MS of complex mixtures with FT-ICR MS at 21 T. We not only employ an established and well-understood chromatographic method that uses columns that separate largely by the aromatic ring number but also provide separation of sulfur types (i.e., thiophene versus sulfide).

Figure 1 shows the summed-ion chromatogram (blue) for all chemical formulas assigned, as well as the summed-ion chromatogram for all unassigned mass spectral peaks (red) for an Arabian heavy vacuum gas oil (HVGO). Greater than 90% of the spectrum relative abundance is assigned in the ring fraction retention time windows and >70% over the entire chromatogram, as shown in SI Figure S1. The chromatogram from LC-MS resembles previous reports for this separation conducted with evaporative light scattering detection (ELSD),[18] with the exception of the saturated hydrocarbon peak. The low peak area for the saturated hydrocarbon peak is due to the decreased ionization efficiency of saturated compounds relative to aromatic compounds by (+) APPI.

https://doi.org/10.1021/acs.analchem.1c01169
Anal. Chem. 2021, 93, 13749−13754

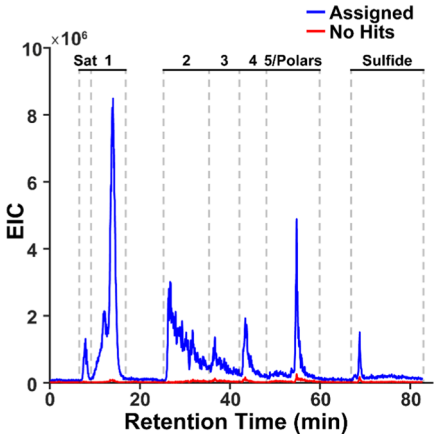

Figure 1. Extracted ion chromatogram of molecular formula assignments (blue) and no hits (red) from the LC-MS analysis of an Arabian HVGO. The majority of the ion current is assigned as molecular formulas with high confidence. The dotted lines indicate the boundaries of the ring fractions and represent the time points over which fractions were collected for direct infusion.

Postcolumn dilution with toluene enables a stable APPI response through the gradient which, combined with automatic gain control (AGC), yields a root-mean-square assignment error below 0.15 ppm over the entire gradient, as shown in SI Figure S2.

The ultra-high resolving power, mass accuracy, and sensitivity of the custom-built 21 T FT-ICR MS provides the most suitable option for the LC-MS analysis of highly complex mixtures such as petroleum. Mass spectra were collected with 3.1 and 6.2 s transient lengths for the LC-MS analysis. Figure 2

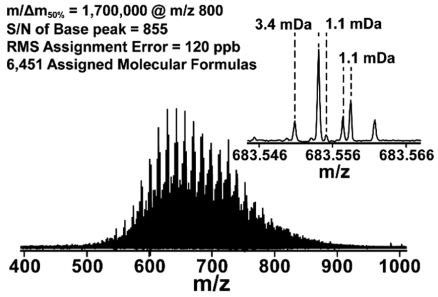

Figure 2. Single scan from the 2-ring elution window of online LC-MS of an Athabasca bitumen heavy distillate. High magnetic field strength enables the analysis of large ion populations for a high dynamic range, high mass accuracy, and high mass resolving power. The common 3.4 and 1.1 mDa mass differences observed in APPI of complex mixtures are baseline resolved across the m/z range of interest.

shows a single scan mass spectrum for a Mackay bitumen heavy distillate (550−600 °C) at a retention time of 27 min. (*i.e.*, from the 2-ring portion of the chromatogram), collected with a 6.2 s transient length. A single absorption mode mass spectrum yields 6451 molecular formula assignments with an RMS error of 0.120 ppm, a mass resolving power of 3 200 000 at m/z 400, and a base peak S/N = 855. A Canadian bitumen heavy distillate was used for this illustration due to its complexity and high abundance of sulfur-containing species. Figure 2 illustrates the performance metrics that the 21 T provides for online analysis of complex mixtures, namely, high dynamic range (and signal-to-noise, S/N) for large ion populations, while retaining high mass accuracy for elemental formula assignment and high mass resolving power.

Data collection of 3.1 s transients ($m/\Delta m_{50\%}$ = 1 600 000 at m/z 400) revealed that the mass resolving power needed to distinguish the 1.1 mDa mass difference was only achieved up to 700 Th. A transient duration of 6.2 s enables resolution of the 1.1 mDa mass difference throughout the mass range of the analysis (approximately m/z 400−1000). The expanded mass segment in Figure 2 shows that both the 1.1 and 3.4 mDa (C_3 versus S_1H_4) mass differences are baseline resolved at m/z 683. For less complex systems, such as the Arabian HVGO discussed in the remainder of the article, the detection period can be shortened to increase the MS sampling rate of the chromatographic peaks while retaining high mass accuracy and mass resolving power sufficient for detailed chemical characterization.

Petroleum characterization is shown here as an example of highly complex samples. However, the mass spectral performance reported is applicable to other systems as well, as has been demonstrated for direct infusion of peptides and recently for matrix-assisted laser desorption (MALDI) imaging of lipids.[19,25] The separation employed, coupled with the current understanding of petroleum chemistry, enables the characterization of complex petroleum samples based on the ring number, heteroatom content, and DBEs.

Comparison with Off-line Direct Infusion Analysis. Fractions were collected offline with a fraction collector, where each individual ring fraction was collected as a single sample. This provided six fractions (*i.e.*, saturates, 1-ring, 2-ring, 3-ring, 4-ring, 5-ring plus polars, and sulfides) for the direct infusion analysis. Table 1 shows the total molecular formula assignments for all fractions by LC-MS, the number of unique assignments in each fraction (as the same m/z is detected over multiple scans by the online method), and the total number of assignments by direct infusion of the collected fractions. Note that the total assignments in the first column highlight the complexity of each mass spectrum, the number of spectra collected across a chromatographic peak, and the ability of the mass spectrometer to provide high resolution/mass accuracy data that facilitate a confident elemental composition assignment. It is not a representation of isomers present or of the number of molecules in the sample. In all fractions, fewer molecular formulas were assigned by the off-line analysis, and

Table 1. Total and Unique Molecular Formulas Assigned by LC-MS and Total Molecular Formula Assignments from Fraction Collection and Direct Infusion of an Arabian HVGO[a]

	total assignments LC-MS	unique assignments LC-MS (per fraction)	total assignments direct infusion
saturates	38 950	3810	1530
1-ring	208 082	7309	3280
2-ring	307 944	7899	4686
3-ring	211 928	6272	3938
4-ring	180 274	6272	4028
5-ring and polars	453 498	11 316	9883
sulfides	385 361	6478	4355
total	**1 786 037**	**49 356**	**31 700**

[a]LC-MS results in more elemental compositions than direct infusion for every fraction.

https://doi.org/10.1021/acs.analchem.1c01169
Anal. Chem. 2021, 93, 13749−13754

compositional changes within ring classes, shown below, were lost. LC-MS analysis reveals molecular classes with low relative abundance (%) that are not observed in the direct infusion analysis. As illustrated in Figure S3 for the 3-ring fraction, the heteroatom class distribution for direct infusion is dominated by sulfur radical cations, whereas lower abundance classes are observed by LC-MS. This suggests that the LC separation reduces ionization suppression effects associated with the direct infusion analysis and that the large ion populations used for LC-MS (enabled by the high magnetic field strength) yield a high dynamic range per single scan. Also, note that a number of newly revealed heteroatom classes contain heavy isotopologues, as expected with the improved dynamic range.

The ring separation used dictates that the same elemental composition observed in different fractions (saturates, 1-, 2-, 3-, 4-, 5+ aromatic ring, and sulfides) is a structural isomer. Furthermore, within each fraction model compounds have chromatographic peak widths of <2 min,[18] so detection of the same elemental composition outside of this window is likely a structural isomer. With a conservative elution time width of 5 min, the total unique assignment (including isomers) from LC-MS of the Arabian HVGO is 79 706. The number of unique values decreases as the elution time window is widened, as shown in SI Figure S4.

Heteroatom and DBE Chromatograms. LC-MS, especially in the case of complex organic mixtures, is a data-rich endeavor. One LC-MS analysis produces ∼600 individual data-containing mass spectra when collecting 6.2 s transients and ∼1200 for 3.1 s transients. For the Arabian HVGO, 1 786 037 molecular formulas were assigned. To better interpret this number of mass spectral peaks, the data can be visualized and examined based on the chemical knowledge gained from molecular formula assignment. The elemental composition enables the assignment of the molecular "class" and the heteroatom content of the molecules other than carbon and hydrogen (e.g., N, O, and S). The summed signal magnitude of each class and the ion accumulation time of each spectrum are used to reconstruct heteroatom class chromatograms that provide information about the composition of a sample across the elution window.

Figure 3 shows heteroatom class chromatograms for the hydrocarbon (HC; only carbon and hydrogen), S_1, and S_2 (top), as well as N_1, N_1O_1, and S_1O_1 (bottom) heteroatom classes from the Arabian HVGO. These chromatograms provide useful insight into the structures observed in each chromatographic peak. For instance, in the trimodal 1-ring peak, hydrocarbons are present throughout the peak; however, the S_1 class is only observed in the latest-eluting portion of the peak. This indicates that the 1-ring sulfur-containing compounds likely reflect a more uniform distribution of structures when compared to the 1-ring hydrocarbons. The differences in structure afforded by the elution time are briefly discussed below and will be the subject of future work. Figure 3 also shows that the saturates through 3-ring classes are comprised primarily of hydrocarbons and sulfur-containing compounds. However, the N_1 class appears in the 4-ring through polar peaks. Similarly, the predominant signals of S_1O_1 and N_1O_1 classes show the importance of oxygen-containing compounds in the polar fraction, likely attributed to sulfoxides and nitrogen heterocycles with a phenol present. Heteroatom class chromatograms also give information regarding the chromatographic features observed within each chromatographic peak. For instance, the 2-ring peak from the total ion

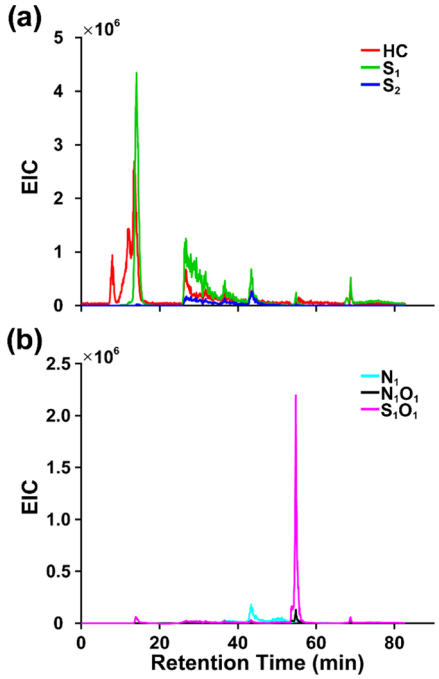

Figure 3. Heteroatom class chromatograms from LC-MS of an Arabian HVGO. (a) Hydrocarbons dominate the saturate fraction and start of the 1-ring fraction, and sulfur-containing species dominate the remaining fractions. (b) Nitrogen-containing species elute in the 4-ring fraction, and polyheteroatomic species elute in the 5-ring and polar fractions.

chromatogram (Figure 1) shows a bimodal distribution with peak maxima at ∼26.5 and 30.5 min. Analysis of the heteroatom class chromatograms reveals that the maximum at ∼30.5 min corresponds primarily to S_1 and S_2 heteroatom classes. This suggests the presence of structural features that are more prevalent for sulfur-containing thiophene-type compounds.

Figure 3 shows both radical and protonated ion types combined, whereas Figure 4 shows the S_1 class separated into radical (red) and protonated (black) species. Although the majority of the chromatogram shows the preference of radical cations over protonated cations, protonated sulfur species are more prominent in the polar spike and sulfide fraction. This

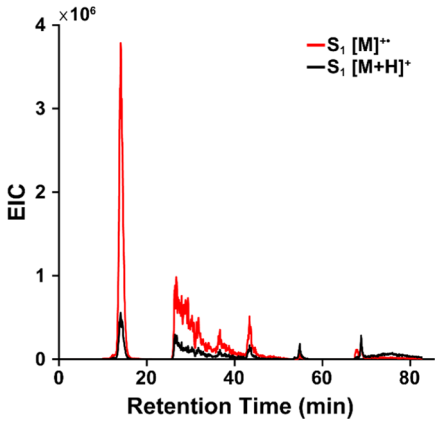

Figure 4. Extracted ion chromatograms for radical and protonated species containing one sulfur heteroatom. Radical ions dominate all fractions until the 5-ring and polars, where protonation is favored.

https://doi.org/10.1021/acs.analchem.1c01169
Anal. Chem. 2021, 93, 13749−13754

indicates that the functionality of the sulfur atom in the polar and sulfide peaks differs from that observed throughout the rest of the chromatogram, where thiophene is the dominant functionality. The ability to generate ion-type specific heteroatom class chromatograms, combined with the knowledge from the chromatographic separation, provides information regarding both the structure and chemical functionality simultaneously.

Fractionation based on the ring number also reveals trends in DBEs. Figure 5 shows selected DBE chromatograms for the

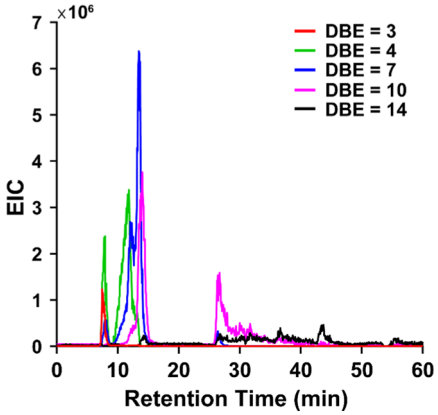

Figure 5. Extracted ion chromatograms for selected DBE values for the hydrocarbon class. Species with DBE = 3 are only detected in the saturate fraction. Aromaticity increases with later eluting fractions. Cycloalkyl ring addition is observed in all fractions.

HC class (no heteroatoms) from the LC-MS analysis. Here, we observe that the compound at DBE = 3 is only observed in the saturated hydrocarbon peak, which is expected since hydrocarbons with one aromatic ring must have a DBE ≥ 4 (benzene ring). The onset of the 1-ring aromatic peak is shown by the DBE = 4 chromatogram. Here, we observe the DBE = 4 compounds in both the saturate and 1-ring aromatic peaks, indicating resolution of structural isomers consisting of four cycloalkyl rings and one aromatic ring. The chromatogram for DBE = 7 shows the onset of 2-ring hydrocarbons, whereas the DBE = 10 and 14 chromatograms show the onset of 3- and 4-ring fractions. Although DBE = 10 is commonly considered to correspond to 3-ring aromatics (*e.g.*, anthracene and phenanthrene), it may also correspond to 4-ring hydrocarbons that contain one phenyl ring and three cyclopenta-1,3-diene rings. Although these five-membered rings are less commonly considered in petroleum structures, a recent molecular imaging work has revealed an abundance of five-membered rings for a wide range of samples.[26]

Finally, DBE trends within ring fractions are revealed. Figure 6 shows a zoomed inset of the 1-ring elution window with EICs of HC compounds with DBE 4−7 (all carbon numbers). Here, we observe that the DBE = 4 compounds are the earliest-eluting, which indicates that alkyl-benzene derivatives show the weakest interaction compared to cycloalkyl-benzene derivatives. This is consistent with model compound results shown previously.[18] The addition of cycloalkane rings to the benzene ring shifts them to a longer retention time, and bimodal distributions are observed for the DBE 5−7 compounds. These are likely isomers in which the cycloalkyl rings are located at different positions relative to the aromatic ring. This level of detail is lost in the off-line direct infusion dataset, as this

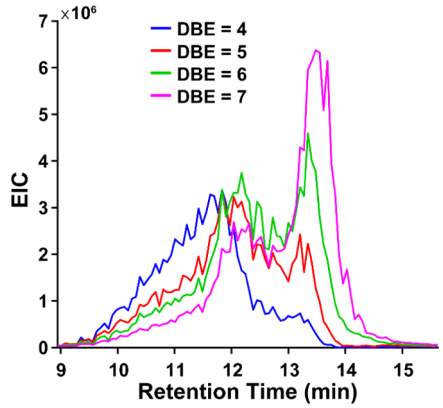

Figure 6. Extracted ion chromatograms from the 1-ring fraction for selected DBE values for the hydrocarbon class. The addition of cycloalkane rings to benzene (DBE = 4) increases the retention time.

portion of the chromatogram is collected as a single fraction. Future work will focus on understanding the structural trends associated with the 1-ring aromatic hydrocarbons.

CONCLUSIONS

Single scan performance at 21 T enables online LC-MS of complex mixtures with unprecedented mass accuracy, mass resolving power, and sensitivity. Accurate mass assignment of elemental compositions exposes chemical class trends by heteroatom content, aromatic ring number, ion type, and structure within a ring class (cycloalkane content). Sample complexity can be used to determine the desired mass resolving power (transient duration), where shorter transients increase the sampling frequency of the chromatographic elution profile. The mass spectral performance reported herein is applicable to other sample types, and applications in environmental remediation (dissolved organic matter and emerging contaminants), lipidomics, and metabolomics are envisioned. Further, the incorporation of tandem MS methods will add additional structural information to these already rich datasets.

ASSOCIATED CONTENT

Supporting Information

The Supporting Information is available free of charge at https://pubs.acs.org/doi/10.1021/acs.analchem.1c01169.

Liquid chromatography conditions; percent relative abundance assigned versus retention time; root-mean-square (RMS) assignment error versus elution time; heteroatom class distribution for the 3-ring fraction by direct infusion and LC-MS; and unique elemental compositions as a function of the elution time window width (PDF)

AUTHOR INFORMATION

Corresponding Author

Ryan P. Rodgers − *National High Magnetic Field Laboratory, Florida State University, Tallahassee, Florida 32310, United States; Future Fuels Institute, Florida State University, Tallahassee, Florida 32310, United States; Department of Chemistry and Biochemistry, 95 Chieftain Way, Florida State University, Tallahassee, Florida 32306, United States;* orcid.org/0000-0003-1302-2850; Phone: (850)-644-

https://doi.org/10.1021/acs.analchem.1c01169
Anal. Chem. 2021, 93, 13749−13754

2398; Email: rodgers@magnet.fsu.edu; Fax: (850)-644-1366

Authors

Steven M. Rowland − *National High Magnetic Field Laboratory, Florida State University, Tallahassee, Florida 32310, United States; Future Fuels Institute, Florida State University, Tallahassee, Florida 32310, United States*

Donald F. Smith − *National High Magnetic Field Laboratory, Florida State University, Tallahassee, Florida 32310, United States;* orcid.org/0000-0003-3331-0526

Gregory T. Blakney − *National High Magnetic Field Laboratory, Florida State University, Tallahassee, Florida 32310, United States;* orcid.org/0000-0002-4205-9866

Yuri E. Corilo − *National High Magnetic Field Laboratory, Florida State University, Tallahassee, Florida 32310, United States; Future Fuels Institute, Florida State University, Tallahassee, Florida 32310, United States*

Christopher L. Hendrickson − *National High Magnetic Field Laboratory, Florida State University, Tallahassee, Florida 32310, United States; Department of Chemistry and Biochemistry, 95 Chieftain Way, Florida State University, Tallahassee, Florida 32306, United States*

Complete contact information is available at: https://pubs.acs.org/10.1021/acs.analchem.1c01169

Author Contributions

‖S.M.R. and D.F.S. contributed equally to this work.

Notes

The authors declare no competing financial interest.

■ ACKNOWLEDGMENTS

A part of this work was performed at the National High Magnetic Field Laboratory ICR User Facility, which was supported by the National Science Foundation Division of Chemistry through DMR-1157490 and DMR-1644779 and the State of Florida.

■ REFERENCES

(1) Qian, K.; Robbins, W. K.; Hughey, C. A.; Cooper, H. J.; Rodgers, R. P.; Marshall, A. G. *Energy Fuels* **2001**, *15*, 1505−1511.
(2) Mediaas, H.; Grande, K. V.; Hustad, B. M.; Rasch, A.; Rueslåtten, H. G.; Vindstad, J. E., *The Acid-IER Method - a Method for Selective Isolation of Carboxylic Acids from Crude Oils and Other Organic Solvents*, International Symposium on Oilfield Scale, 2003; p 7.
(3) Rowland, S. M.; Robbins, W. K.; Corilo, Y. E.; Marshall, A. G.; Rodgers, R. P. *Energy Fuels* **2014**, *28*, 5043−5048.
(4) Putman, J. C.; Rowland, S. M.; Corilo, Y. E.; McKenna, A. M. *Anal. Chem.* **2014**, *86*, 10708−10715.
(5) Lobodin, V. V.; Robbins, W. K.; Lu, J.; Rodgers, R. P. *Energy Fuels* **2015**, *29*, 6177−6186.
(6) Vasconcelos, G. A.; Pereira, R. C. L.; Santos, C. dF.; Carvalho, V. V.; Tose, L. V.; Romão, W.; Vaz, B. G. *Int. J. Mass Spectrom.* **2017**, *418*, 67−72.
(7) Oro, N. E.; Lucy, C. A. *Energy Fuels* **2013**, *27*, 35−45.
(8) Cho, Y.; Na, J.; Nho, N.; Kim, S.; Kim, S. *Energy Fuels* **2012**, *26*, 2558−2565.
(9) Nyakas, A.; Han, J.; Peru, K. M.; Headley, J. V.; Borchers, C. H. *Environ. Sci. Technol.* **2013**, *47*, 4471−4479.
(10) Podgorski, D. C.; Corilo, Y. E.; Nyadong, L.; Lobodin, V. V.; Bythell, B. J.; Robbins, W. K.; McKenna, A. M.; Marshall, A. G.; Rodgers, R. P. *Energy Fuels* **2013**, *27*, 1268−1276.
(11) Robson, W. J.; Sutton, P. A.; McCormack, P.; Chilcott, N. P.; Rowland, S. J. *Anal. Chem.* **2017**, *89*, 2919−2927.
(12) Lababidi, S.; Panda, S. K.; Andersson, J. T.; Schrader, W. *Anal. Chem.* **2013**, *85*, 9478−9485.
(13) Lababidi, S.; Schrader, W. *Rapid Commun. Mass Spectrom.* **2014**, *28*, 1345−1352.
(14) Ghislain, T.; Guricza, L. M.; Schrader, W. *Rapid Commun. Mass Spectrom.* **2017**, *31*, 495−502.
(15) Molnárné Guricza, L.; Schrader, W. *J. Chromatogr. A.* **2017**, *1484*, 41−48.
(16) Gavard, R.; Jones, H. E.; Palacio Lozano, D. C.; Thomas, M. J.; Rossell, D.; Spencer, S. E. F.; Barrow, M. P. *Anal. Chem.* **2020**, *92*, 3775−3786.
(17) Smith, D. F.; Podgorski, D. C.; Rodgers, R. P.; Blakney, G. T.; Hendrickson, C. L. *Anal. Chem.* **2018**, *90*, 2041−2047.
(18) Putman, J. C.; Rowland, S. M.; Podgorski, D. C.; Robbins, W. K.; Rodgers, R. P. *Energy Fuels* **2017**, *31*, 12064−12071.
(19) Hendrickson, C. L.; Quinn, J. P.; Kaiser, N. K.; Smith, D. F.; Blakney, G. T.; Chen, T.; Marshall, A. G.; Weisbrod, C. R.; Beu, S. C. *J. Am. Soc. Mass Spectrom.* **2015**, *26*, 1626−1632.
(20) Kaiser, N.; Savory, J.; Hendrickson, C. *J. Am. Soc. Mass Spectrom.* **2014**, *25*, 943−949.
(21) Boldin, I. A.; Nikolaev, E. N. *Rapid Commun. Mass Spectrom.* **2011**, *25*, 122−126.
(22) Blakney, G. T.; Hendrickson, C. L.; Marshall, A. G. *Int. J. Mass Spectrom.* **2011**, *306*, 246−252.
(23) Xian, F.; Hendrickson, C. L.; Blakney, G. T.; Beu, S. C.; Marshall, A. G. *Anal. Chem.* **2010**, *82*, 8807−8812.
(24) Corilo, Y. E. *PetroOrg Software*; Florida State University: Omics LLC: Tallahassee, FL, 2014.
(25) Bowman, A. P.; Blakney, G. T.; Hendrickson, C. L.; Ellis, S. R.; Heeren, R. M. A.; Smith, D. F. *Anal. Chem.* **2020**, *92*, 3133−3142.
(26) Schuler, B.; Meyer, G.; Peña, D.; Mullins, O. C.; Gross, L. *J. Am. Chem. Soc.* **2015**, *137*, 9870−9876.